Journal of Microscopy and Ultrastructure 3 (2015) 120–136

Contents lists available at ScienceDirect

Journal of Microscopy and Ultrastructure

journal homepage: www.elsevier.com/locate/jmau

Experimental Study

Can vitamin C affect the $KBrO_3$ induced oxidative stress on left ventricular myocardium of adult male albino rats? A histological and immunohistochemical study

Mohammad E.E. El-Deeb[a], Amal A.A. Abd-El-Hafez[b,*]

[a] *Anatomy Department, Egypt*
[b] *Department of Histology, Faculty of Medicine, Tanta University, El Geesh street, Tanta, Egypt*

ARTICLE INFO

Article history:
Received 29 November 2014
Received in revised form 10 February 2015
Accepted 9 March 2015
Available online 17 March 2015

Keywords:
Potassium bromate
Cardiotoxicity
Vitamin C
Antidote
Ultrastructurally

ABSTRACT

Potassium bromate ($KBrO_3$) cardiotoxicity is not widely recognized, in spite of its well known oxidative cell and tissue damage. The wide exposure to $KBrO_3$ in food and water necessitates finding of a simple and available antidote for its hazards like vitamin C. There are growing evidences that the regulation of redox reactions in cells is intimately tied to the levels of antioxidants. As the heart is highly vulnerable for oxidative damage, left ventricle muscle was the spotlight of our study. For this purpose 20 adult male albino rats were categorized into four groups (five rats each). Group 1 served as control; group 2 received 30 mg/kg/day vitamin C for 4 weeks. Group 3 was injected intraperitoneally with $KBrO_3$ 20 mg/kg/dose twice weekly for 4 weeks, and group 4 received both vitamin C and $KBrO_3$ in the same scheme. Heart specimens were processed for various histological examinations. Sections from $KBrO_3$ treated animals showed focal disruption of cardiac myocytes, deeply stained nuclei and dilated congested blood vessels. Ultrastructurally, irregular indented nuclei, focal lysis of the myofibrils and swelling of mitochondria were also observed. In contrast, minimal changes were observed in rats treated concomitantly with both vitamin C and $KBrO_3$. Caspase 3 immunohistochemical reaction was nonsignificantly increased in group 3 cardiomyocytes. Semiquantitative morphological mitochondrial scoring and statistical analyses revealed significant changes between the studied groups. Finally, $KBrO_3$ induced structural changes in rat cardiac muscle could be ameliorated by concomitant treatment with vitamin C.

1. Introduction

Fruits and vegetables supply more than 90% of the vitamin C in human diets. Except human, most of the higher animals can synthesize vitamin C (L-ascorbate) [1].

The biological role of ascorbate is to act as a reducing agent, donating electrons to various enzymatic and a few non-enzymatic reactions. Being an essential co-factor for many enzymes, vitamin C is required for the prevention of scurvy and maintenance of healthy skin, gums and blood vessels. It helps in the formation of collagen, absorption of inorganic iron, reduction of plasma cholesterol level, inhibition of nitrosoamine formation and enhancement of the immune system; simply it is essential for healthy life [2].

Furthermore, being an efficient scavenger of reactive oxygen species (ROS) and free radicals, vitamin C exerts a protective role against many environmental carcinogenic compounds and even some types of cancer [3].

* Corresponding author. Tel.: +20 403357557; fax: +20 403339604.
E-mail address: amalmb1991@hotmail.com (A.A.A. Abd-El-Hafez).

http://dx.doi.org/10.1016/j.jmau.2015.03.003
2213-879X/

Vitamin C as an antioxidant; it protects the body against oxidative stress damage to the important biological macromolecules, such as DNA, proteins, and lipids [3]. Its daily adult requirements are 90–120 mg; that is nearly found in four moderate sized lemons or tomatoes or else in three moderate sized oranges or strawberries [3].

Potassium bromate ($KBrO_3$) is a food additive used primarily as a dough conditioner for flour. It is also generated as a contaminant in drinking water managed with ozone as a disinfectant [4,5]. In addition, $KBrO_3$ is used in hair lotions, fish paste and fermented beverages [6].

Several reports on the assessment of potassium bromate danger show that it is highly toxic as it causes lipid peroxidation and oxidative DNA damage [6]. Oral doses of 185–385 mg/kg body weight results in irreversible toxic effects on body systems. The LD50 (median lethal dose, 50%) of potassium bromate was reported to be 157 mg/kg bodyweight, while lower doses are associated with vomiting, diarrhea, nausea and abdominal pain [7–9].

$KBrO_3$ was considered unsafe and banned from the list of food additives by many countries [10].

However since 1991 the FDA (Food and Drug Administration) has urged bakers to stop using it; furthermore, many trials are carried out for its prevention in water [11]. In our country it is still used in backing, and is generated as a contaminant in drinking water treated with ozone as disinfectant; up till now it is difficult to be avoided so it was compulsory to discover simple antidote for it.

The heart is a vital organ that has about 40% of its volume mitochondria [12], which are the organelles for cell respiration (aerobic respiration). Mitochondria oxidize the major products of glucose, pyruvate, and NADH (nicotinamide adenine dinucleotide hydride), in the presence of oxygen. This pushed us to select the cardiac muscle as an expected vulnerable target for the oxidative damage of the $KBrO_3$, together with the very scarce studies in this concept. Mitochondria play an important role in apoptosis under a variety of proapoptotic conditions, such as oxidative stress by release of its cytochrome c which is a key event in the activation of caspase 3 induced apoptosis [13]. So assessment of apoptosis is considered to be an indicator of cardiac stress. "Thus, the aim of this work was to ascertain the role of ascorbic acid present in fruits or juices as a natural antioxidant to inhibit the toxic effects of $KBrO_3$ on the left ventricular cardiac muscle, using histological and immunohistochemical assessments."

2. Materials and methods

2.1. Preparation of animals and study design

Twenty adult male albino rats, weighed between 200 and 230 g, were used in this study. They were housed under similar conditions in clean ventilated stainless steel cages and had good supply of food and water throughout the experiment. The animals were divided into four groups of five rats each:

Group 1: Served as a control group and rats did not receive any medications.

Group 2: Rats were given vitamin C orally.

Group 3: Rats were given $KBrO_3$ intraperitoneal (IP)

Group 4: Rats were given both $KBrO_3$ (IP) and oral vitamin C concomitantly.

2.2. $KBrO_3$ and vitamin C paperwork

$KBrO_3$ used was purchased from Sigma Chemicals (Sigma, St Louis, MO, USA), while the vitamin C was in the form of Cevarol oral drops (CID, Cairo, Egypt).

$KBrO_3$ was injected (IP) (groups 3 and 4) at a toxic dose of 20 mg/kg body weight/dose twice weekly for 4 weeks prepared as 40 mg/ml of distilled water [14]. The vitamin C was given orally (groups 2 and 4) in a high dose of 30 mg/kg/day; the dose was divided twice daily [3], for 4 weeks concomitant with $KBrO_3$.

2.3. Acquiring and processing of specimens

At the correct time, all animals were sacrificed under anesthesia and the thorax was opened, the left ventricle was extracted on the proper fixative and cut into small pieces, then immersed in the fixative till processing. All procedures on animals followed the guidelines for work on experimental animals approved by Ethical Committee of Faculty of Medicine in Tanta University.

2.3.1. Light microscopy examination

The specimens were immersed in 10% neutral-buffered formalin for 24 h, washed, dehydrated cleared and paraffin immersed. Then, 5 μm sections were stained with hematoxylin/eosin (H&E) and Mallory's trichrome stains and examined by microscopically [15].

2.3.2. Semithin and ultrathin sections examination

Small pieces of the tissues were fixed in 2% paraformaldehyde and 2% glutaraldehyde solution in 0.1 M phosphate buffer pH 7.2 and kept in the fridge overnight, rinsed in 0.1 M phosphate buffer and post-fixed in phosphate-buffered 1% osmium tetroxide for 1 h. Subsequently, the specimens were washed in buffer, dehydrated in a graded series of ethanol solutions, passed through propylene oxide.

Semithin sections (1 μm thick) were cut with ultramicrotome and then stained with 1% toluidine blue and examined by light microscope for proper orientation and imaging.

Ultrathin sections (80–90 nm) were cut on ultramicrotome, stained with 8% of uranyle acetate followed by lead citrate to be examined by (JEM 100 S transmission electron microscope (UK) (Ltd) at 80 kV in the EM unit, Faculty of Medicine, Tanta University) [16].

2.3.3. Immunohistochemical detection of myocyte-specific caspase 3 reaction

The reaction was detected using an anti-caspase 3 antibody (Ab). Sections were incubated with the primary rabbit anti-caspase 3 antibody (R&D Systems, Minneapolis, MN, USA) overnight at 4 °C. Primary Ab binding was detected using a horseradish peroxidase-conjugated goat anti-rabbit antibody (Vector Laboratories, Burlingame, CA, USA) and visualized by development with

3,3′-diaminobenzidine (DAB, Sigma). All sections were counterstained with hematoxylin. It appears as zymogen granules in the cytoplasm and partially on the nucleus [17,18].

2.4. Quantitative mitochondrial morphological scoring

A semiquantitative evaluation of 20 electron microscopic non-overlapped fields at 2000×–3000× magnifications was conducted for each specimen. The scoring method used in this evaluation was adapted according to Bishop et al. [19] and included four grades as follows:

Grade 0: no evidence of cellular pathology or early autolysis, or an occasional mitochondrion with minimal loss of cristae while the remainder of mitochondria appear normal; *Grade 1*: discontinuous cristal membranes and/or partial loss of cristae and matrix material in a few mitochondria; *Grade 2*: multiple disruptions of the cristal membrane and substantial loss of cristae and matrix in approximately half of the mitochondria; *Grade 3*: fragmented cristal membranes and effacement of central architecture in a majority of the mitochondria.

After analysis for the degree of mitochondrial morphological changes, the mean of the observations was recorded and the grading data were subjected to statistical analysis.

This score was called semiquantitative as the mitochondrial alterations were not recorded in count one-by-one but were assessed in fields.

2.5. Morphometric analyses

In each group, different Mallory's trichrome-stained sections were examined for mean total optical density. The collagen greenish-blue color was measured in five different fields for each slide. The mean total optical density was used by the same maneuver to measure the caspase 3 brown reaction. Measurements were taken using a Leica Qwin V3 software program (Leica Geosystems) Switzerland, connected to a microscope (Leica Microsystem, Heerbrugg, Switzerland).

2.6. Statistical analyses

Statistical analyses were done using Statistical Package for the Social Sciences (SPSS) (Hong Kong) Ltd., Westlands Centre, China for detecting the significance of the score to assess mitochondrial morphological grading using Kruskal–Wallis test while comparing for the significance between groups we used Mann–Whitney test. The significance of optical density for Mallory's trichrome stained sections and caspase 3 reaction was measured by (ANOVA).

3. Results

This study was carried out on twenty animals.

3.1. Light microscopy

3.1.1. Hematoxylin and eosin (H&E) and toluidine blue stained sections

In both control and vitamin C treated groups (groups 1 and 2), the left ventricular myocardial structure was alike. At H&E and semithin sections, the muscle fibers were mostly long cylindrical cells with one or two, large, oval centrally located nuclei and in H&E sarcoplasm was acidophilic (Fig. 1a–c). There were paler stained regions around the nucleus (Fig. 1a). The cells were branched and re-anatomizing to each other, giving the impression of a continuous three-dimensional cytoplasmic network, syncytium (Fig. 1a, b). In semithin sections, striations were obviously seen (Fig. 1d, e). Dark-staining transverse lines that cross the chains of cardiac cells at irregular intervals (intercalated disks) may appear as straight lines or may exhibit a steplike pattern (Fig. 1d, e).

Between the muscle fibers, delicate sheaths of collagenous endomysial connective tissue and cells supported the extremely rich capillary network (Fig. 1c–e).

In $KBrO_3$ received group (group 3) : the cardiomyocytes together with the surrounding connective tissue and the capillary network showed various degrees of structural changes. In some occasions the cardiomyocyte had partially disintegrated cytoplasm with widened juxtanuclear paler stained area and darker nuclei (Fig. 2a, b). Sometimes it possessed spherical deeply stained nuclei instead being cylindrical vesicular like in other adjacent cells (Fig. 2c). In other areas, the nuclei of some cardiomyocytes were huge and less elongated (Fig. 2d). Cardiac muscle cells may lose striations and had globular cytoplasm (Fig. 3a). Collagen bundle was seen, only once replacing a part of a myocyte (Fig. 3b). Connective tissue matrix was abundant in between myocytes in some sections (Fig. 3b, c); its cells were more abundant than the myocytes in other sections (Fig. 4a), further regions showed congested capillaries or extravasated blood cells (Figs. 3b, d and 4b, c).

The changes in myocardium of concomitantly $KBrO_3$ and vitamin C treated group (group 4) were noticeably less than in group 3. Most of the cardiac muscle fibers appeared cylindrical, branching, and anastomosing having central oval vesicular nuclei (Fig. 5a, b). Meanwhile, few cardiac myocytes showed focal areas of pale sarcoplasm and noticeably increased nuclei of the fibroblasts in some sections (Fig. 5a, b). In addition, mild congestion of blood vessels and abundant connective tissue matrix was observed in between the cardiac muscle fibers (Fig. 5a, d). The globular cytoplasmic disintegration became limited to parts of the sarcoplasm and did not diffuse in the entire of the myocyte (Fig. 5c).

3.1.2. Mallory's trichrome stained sections

Cardiac myocytes of left ventricular sections from both nontreated and vitamin C treated control groups showed few collagen fibers between the cardiac muscle fibers and around blood vessels (Fig. 6a, b). Sections from the $KBrO_3$ treated group (group 3) revealed obvious increase in the collagen fibers, which appeared as dense, wavy, thick bundles in between the cardiac muscle fibers (Fig. 7a, b). Other sections showed focal areas of collagen fibers replace some

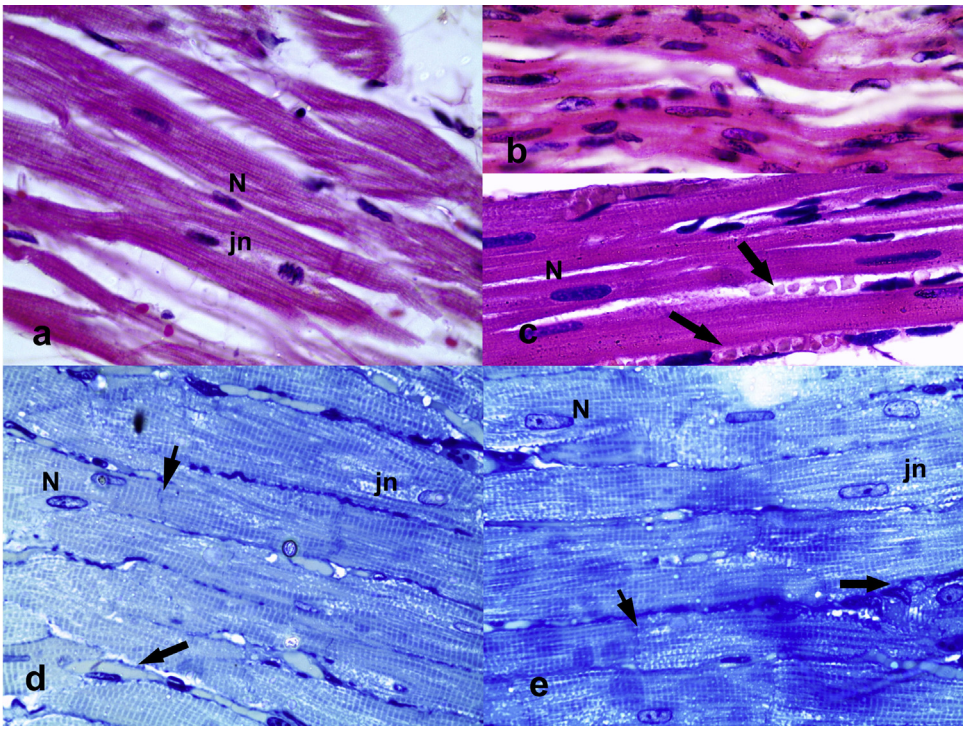

Fig. 1. Photomicrographs of control left ventricle muscle sections showing cylindrical muscle fibers have acidophilic sarcoplasm (a–c), large, oval centrally located vesicular nucleus (N) (a–e), paler stained regions around the nucleus (juxta nuclear) (jn) in (a). The branched fibers abut with each other giving the impression of a continuous three-dimensional cytoplasmic network in (a, b). In semithin sections (c, d) the striations are obvious, intercalated disks are straight lines (thin arrows) and paler stained regions around the nucleus (jn). Delicate sheaths of collagenous connective tissue supported the extremely rich capillary network (thick arrows) (c–e). (Groups 1 and 2) (a–c) H&E 1000× and (d, e) toluidine blue 1000×.

degenerated parts of the cardiac muscle fibers (Fig. 7c, d). Sections from rats of the $KBrO_3$ and vitamin C treated group (group 4) showed few collagen fibers between the regularly arranged cardiac muscle fibers was little than group 3, especially adjacent to the blood vessels (Fig. 8a–d).

3.1.3. *Immunohistochemical detection of myocyte-specific caspase 3 reactions*

The reaction appeared as (brown zymogen granules) represents Ab binding sits, contrasted against a blue hematoxylin background. No apparent difference was detected in the myocytes reactions of control and vitamin C received animals (groups 1 and 2) (Fig. 9a, b); however an apparent slight increase in the reaction was detected in the left ventricular myocytes after $KBrO_3$ administration (group 3) (Fig. 9c). When vitamin C was administered with $KBrO_3$ (group 4), the reaction was somewhat bright (Fig. 9d).

3.2. *Electron microscopy*

The electron microscopic examination of myocardial sections obtained from control and vitamin C treated groups (groups 1 and 2) revealed similar structures. Each cardiac myocyte contained a central oval euchromatic nucleus with a prominent nucleolus (Fig. 10a, b).

The sarcoplasm, in longitudinal sections, was composed of longitudinal arrays of cylindrical myofibrils that separate to pass around the nucleus, thus outlining a biconical juxtanuclear region in which the cell organelles were concentrated. This region was rich in mitochondria and glycogen (Fig. 10b, c). In addition to the juxtanuclear mitochondria, cardiac muscle cells possessed large mitochondria that were densely packed between the myofibrils and often a single mitochondrion extent the full length of a sarcomere. They contained numerous, closely packed cristae (Figs. 10b, c and 11a, b). Concentrations of glycogen granules were also located between the myofibrils (Fig. 10a, b). Sarcomeres presented between two successive Z lines composed of dark bands (A bands) and two hemilight bands (I bands). The center of each A band was occupied by a pale area, the H band, which was bisected by a thin M line. Diads were present at the level of Z lines (Fig. 10d). Lace-like profiles of sarcoplasmic reticulum and parts of T tubules can be identified; sarcolemmal invaginations by the T tubules at the Z lines levels were obvious (Fig. 11a–d).

Intercalated disks had transverse portions, where fasciae adherens and desmosomes were abundant, as well as longitudinal portions rich in gap junctions. On the cytoplasmic aspect of the sarcolemma of intercalated disks, thin myofilaments attach to the fasciae adherens, which are thus analogous to Z disks (Fig. 11d).

In $KBrO_3$ treated group (group 3), electron microscopic examination of the myocardium showed that the nuclei of some myocytes appeared irregular while others were deeply indented with clumps of heterochromatin and widening of the juxtanuclear region in most of them (Fig. 12a, b). Moreover, focal areas of fragmentation and lysis of the myofibrils were observed in some myocytes,

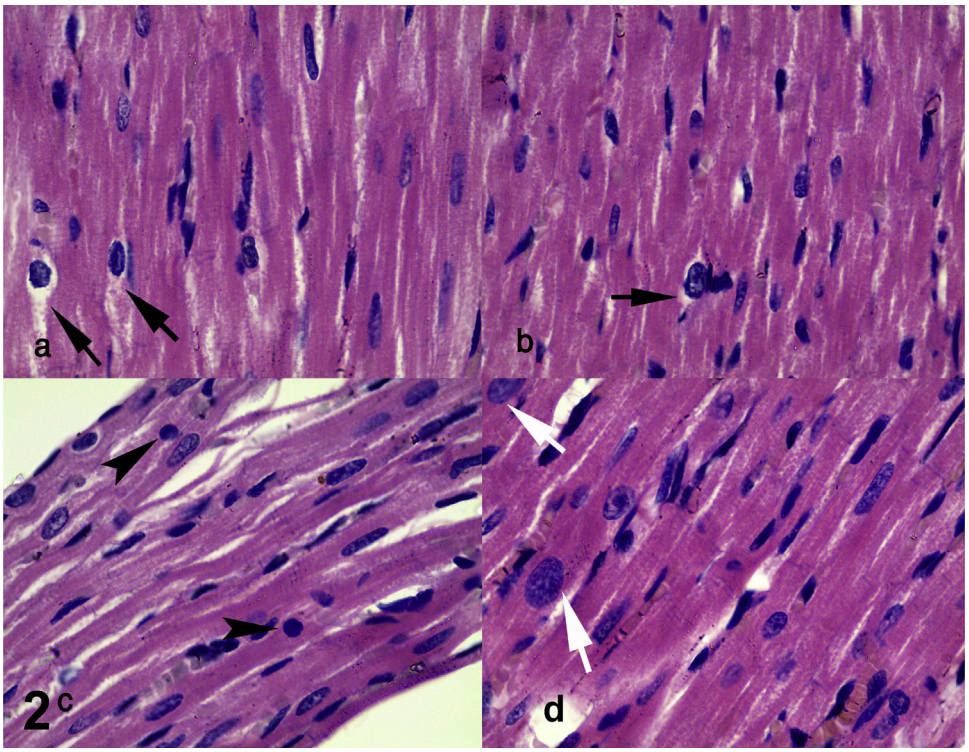

Fig. 2. Photomicrographs of left ventricle muscle sections of rats treated with $KBrO_3$ showing disintegrated cardiac muscle cells with deeply stained nuclei and widened juxtanuclear paler stained region (arrows) (a, b), spherical deeply stained nuclei (arrow heads) instead being cylindrical vesicular like in adjacent cells in (c) and huge and less elongated nuclei (white arrows) in (d). (Group 3) H&E 1000×.

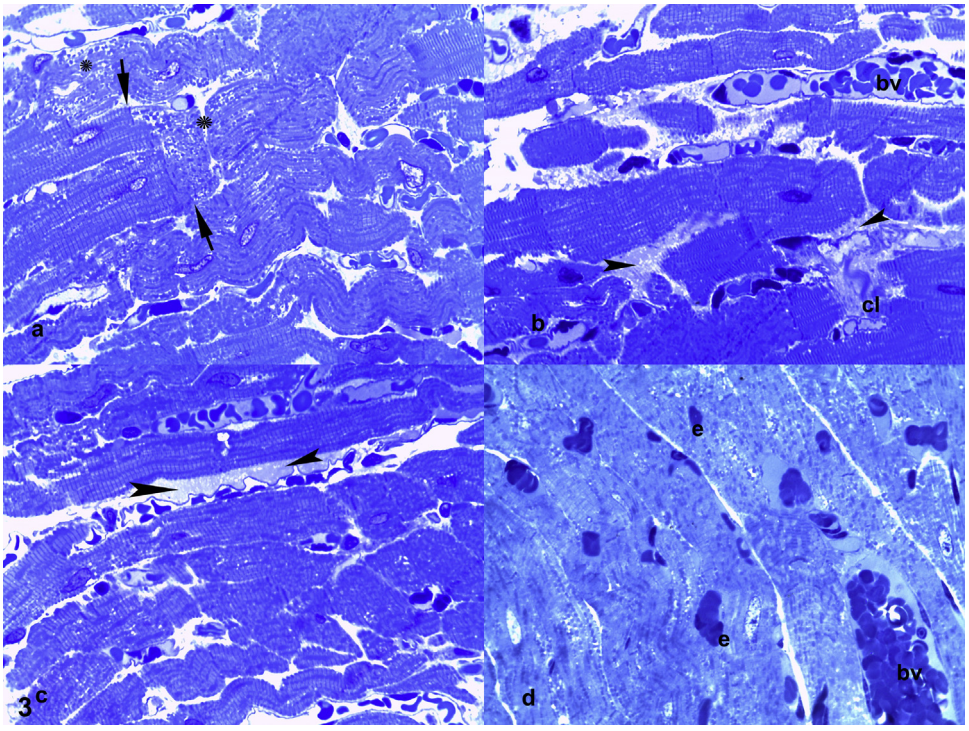

Fig. 3. Semithin sections of left ventricle muscle of $KBrO_3$ treated rats showing some corrugated cardiac muscle cells with lost striations, disintegrated globular cytoplasm (stars) side to side with apparently normal cells and separated from each by intercalated disks (arrows) in (a). Collagen bundle (cl) replacing part of a myocyte and dilated congested blood vessels (bv) in (b). Connective tissue matrix is abundant in between myocytes (arrow heads) in (b, c). Other regions show congested capillaries (bv) or extravasated blood cells (e) between myocytes in (b, d). (Group 3) Toluidine blue 1000×.

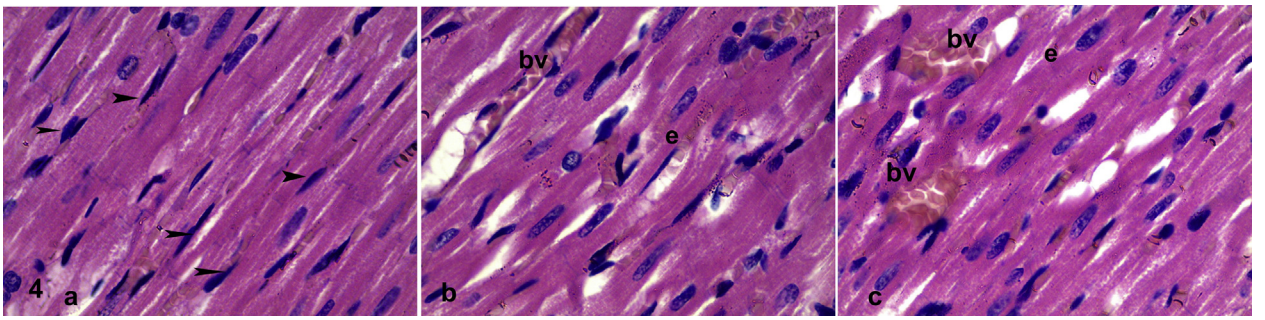

Fig. 4. Photomicrographs of left ventricle muscle sections of rats treated with $KBrO_3$ showing connective tissue cells are more abundant than the myocytes (arrow heads) in (a) congested capillaries (bv) and extravasated blood cells (e) in (b, c). (Group 3) H&E 1000×.

with disruption of myofibrils (Fig. 13a–d). In most of the cells there was loss of the uniform thickness pattern of myofibrils, wherein some appeared very thin but others were average, and several were split (Fig. 14a–d). Areas of sarcoplasmic vacuolization, especially in the juxtanuclear region were seen (Figs. 14b and 15a). The mitochondria were irregularly arranged with different sizes and have heterogenous density of the matrix. Sometimes it appeared swollen, and with partially destructed cristae (Figs. 13a–d and 15a–d). Intercalated disks and sarcoplasmic reticulum did not appear to be distorted (Figs. 13–15) while glycogen granules were slightly depleted (Fig. 15b, d).

In $KBrO_3$ and vitamin C treated group (group 4), all ultrathin sections showed an almost better appearance of cardiac muscle fibers than in group 3. The nuclei of the myocytes appeared oval euchromatic with average juxtanuclear region, while others were eccentric, slightly irregular with a prominent nucleolus (Fig. 16a, b). The myofibrils were nearly regularly arranged showing an average size and regular striation pattern (Fig. 16c, d). Most of the mitochondria retained their intact cristea and dense matrix while few appeared swollen with irregular shape, size and partially destroyed cristae or central effacement (Figs. 16c–e, 17a–d and 18). Intercalated disks appeared to be intact in longitudinal and transverse sections (Fig. 17a,

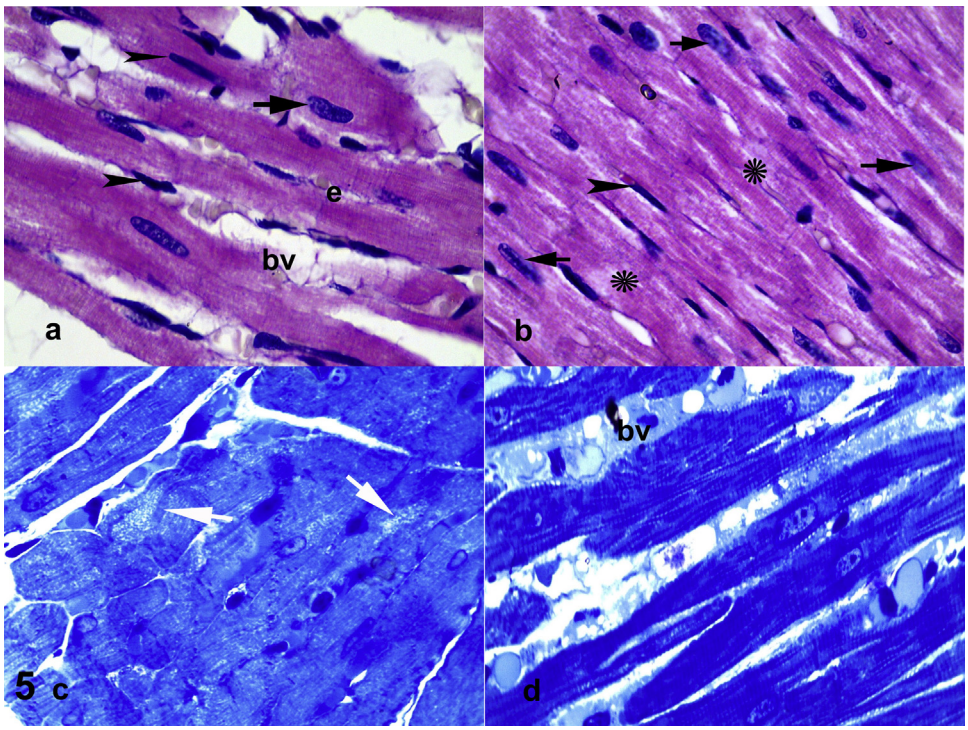

Fig. 5. Photomicrographs of left ventricle muscle sections of rats treated with $KBrO_3$ and vit. C showing most of the cardiac muscle fibers appear cylindrical, branching, and anastomosing having central oval vesicular nuclei (arrows) (a, b), some show focal areas of pale sarcoplasm (stars) and the nuclei of the fibroblasts (arrow heads) are abundant (a, b). Congested capillaries (bv) or extravasated blood cells (e) and abundant connective tissue matrix are observed in between the cardiac muscle fibers (a, d). The globular cytoplasmic disintegration is limited to parts of the sarcoplasm (white arrows) (c). (Group 4) (a) H&E 1000×, (b) H&E 400×, and (c, d) toluidine blue 1000×.

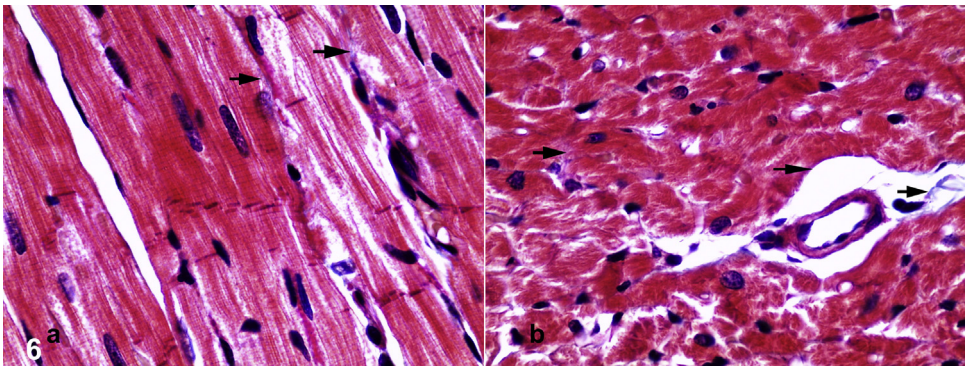

Fig. 6. Photomicrographs of control left ventricle muscle sections showing few collagen fibers between the cardiac muscle fibers and around blood vessels (arrows) in the LS (a) and TS (b) sections of left ventricular muscle. (Group 2) Mallory's trichrome 1000×.

b). The dot-like regular lattice representing the contractile proteins of the sarcomeres with the thick filaments surrounded by thin filaments were unchanged in transverse sections (Fig. 17a).

Regarding the T tubules and sarcoplasmic reticulum they were slightly dilated in some sections and average in others, as well as the still depleted glycogen (Fig. 18a, b).

3.3. Statistical analyses

3.3.1. Quantitative mitochondrial morphological changes evaluation

The semiquantitative evaluation of mitochondrial morphological changes indicated that control animals (groups 1 and 2) generally exhibited mitochondrial alterations that ranged from grade 0 to 1, whereas mitochondria in $KBrO_3$ treated animals (group 3) showed alterations generally in the 2-to-3-grade range. When vit. C was added in the way of $KBrO_3$ (group 4) the alterations were shifted to the 1-to-2-grade range. Since variability existed from region to region within the individual animal, grading reflected the overall assessment of damage for each animal. In addition the analysis signified the use of this score in grading assessments.

For simplicity of presentation, the score grading for mitochondrial morphological changes was summarized in Table 1 indicating significant damage between the controls and $KBrO_3$ treated groups, however the hurt was dropped

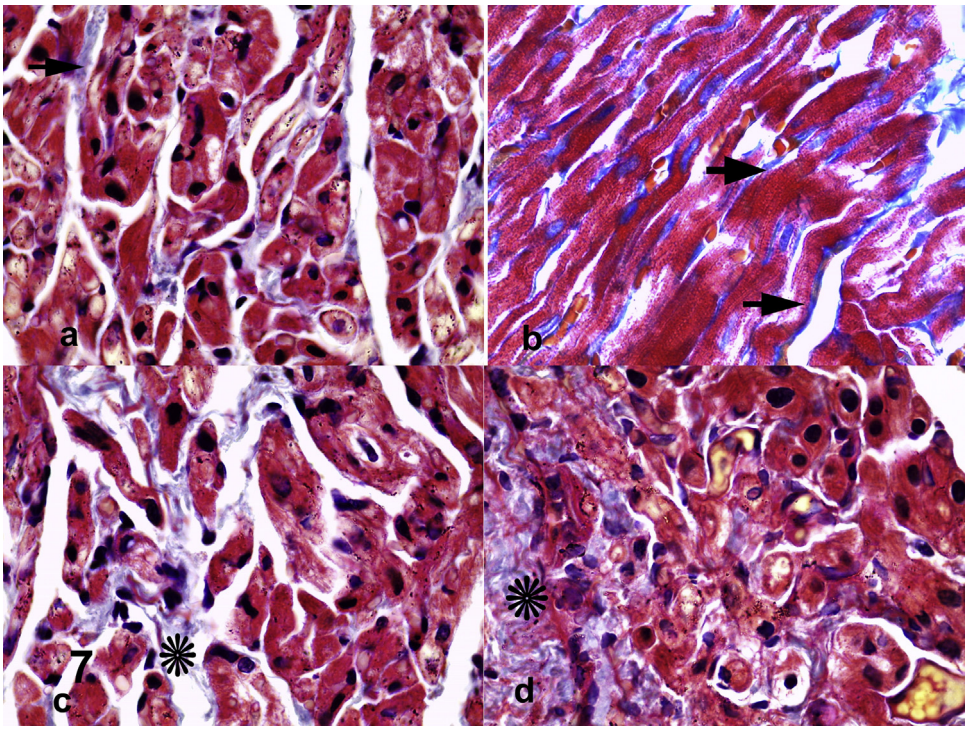

Fig. 7. Photomicrographs of left ventricle muscle sections of rats treated with $KBrO_3$ showing large amount of collagen fibers, TS in (a), LS in (b) which appear as dense, wavy, thick bundles in between the cardiac muscle fibers (arrows). Focal areas of collagen fibers (stars) replace some degenerated parts of the cardiac myocytes (c, d). (Group 3) Mallory's trichrome 1000×.

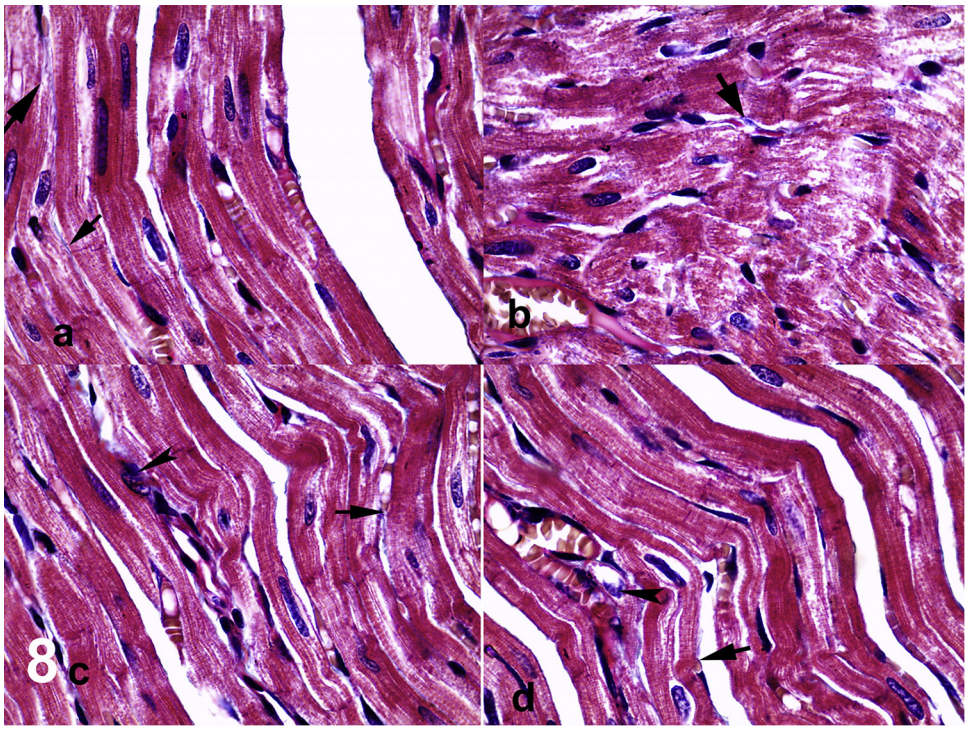

Fig. 8. Photomicrographs of left ventricle muscle sections of rates treated with $KBrO_3$ and vit. C showing collagen fibers seen between the organized regularly arranged cardiac muscle fibers (arrows a–d) and adjacent to the blood vessels (arrow heads) in (c, d). (Group 4) Mallory's trichrome 1000×.

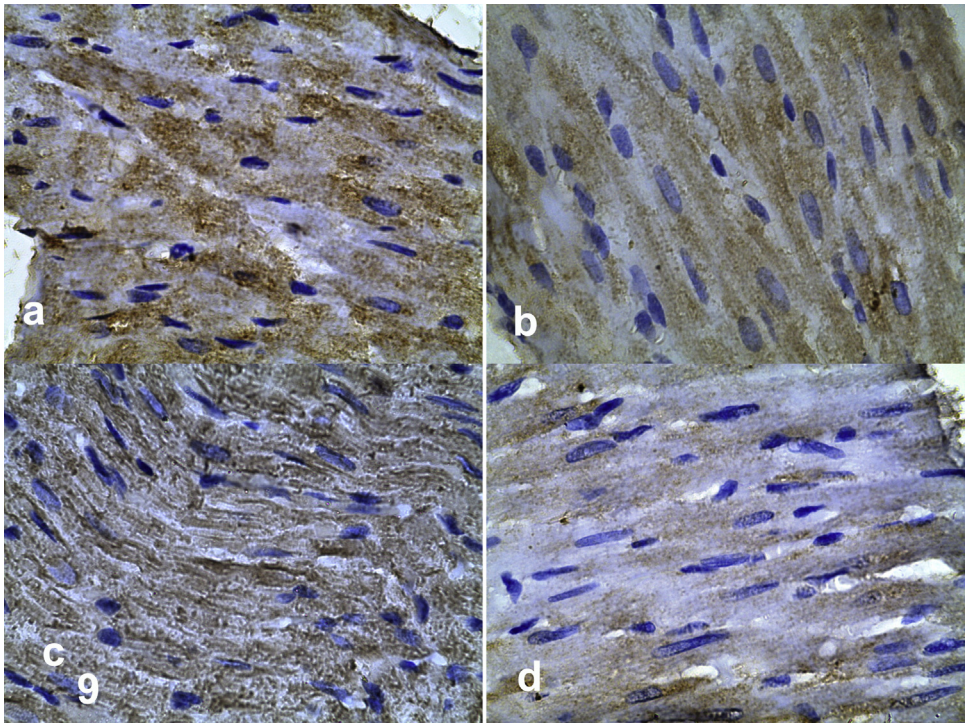

Fig. 9. Photomicrographs of left ventricle muscle sections showing that the brown (DAB) staining (appears as zymogen granules) represents Ab binding sits, contrasted against a blue (hematoxylin) background. Anti-caspase 3 Ab and hematoxylin. (Groups 1 and 2) (a, b), (group 3) (c), and (group 4) (d) 1000×.

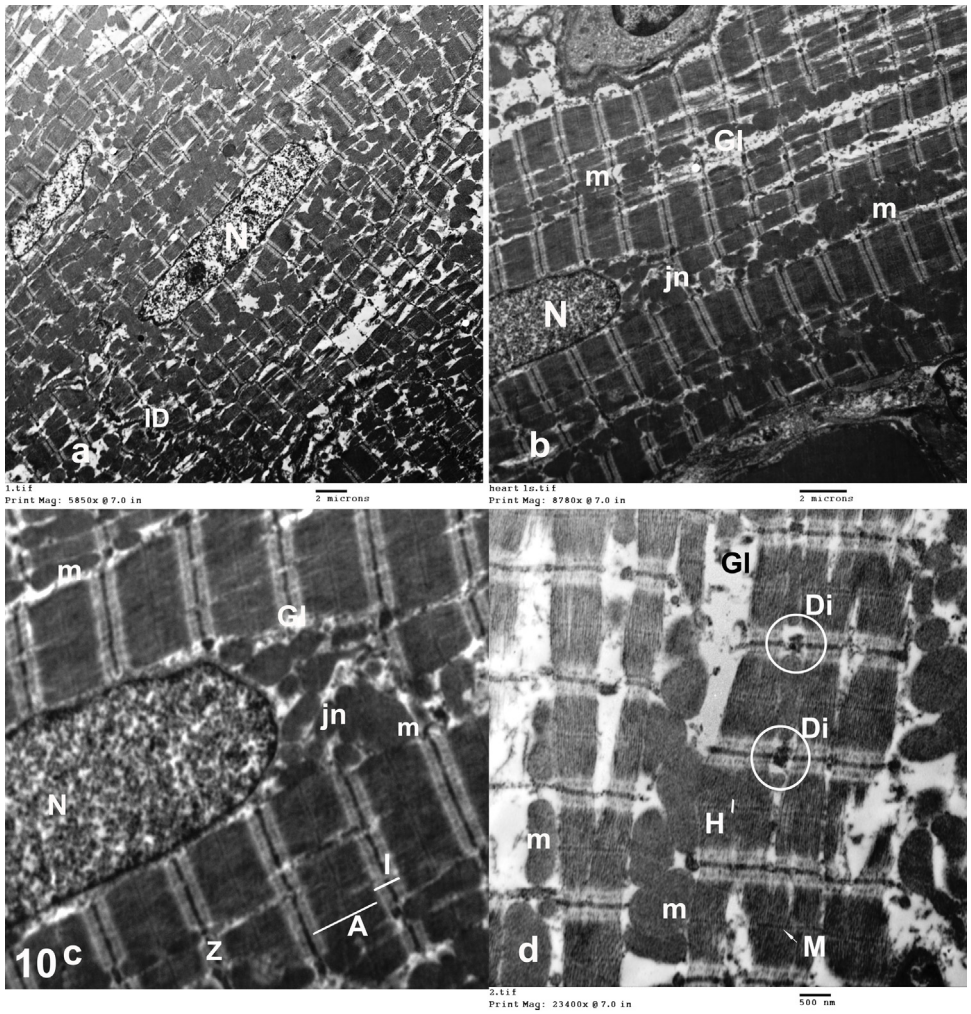

Fig. 10. Electronmicrographs of control left ventricle muscle sections showing longitudinal sections of cardiac myocytes; each contains a single oval euchromatic nucleus (N) in (a–c) with a prominent nucleolus in (a). The sarcoplasm is composed of longitudinal arrays of cylindrical myofibrils pass around the nucleus, outlining a juxtanuclear region (jn) rich in mitochondria (m) and glycogen (Gl), which are also located between the myofibrils (b–d). Large mitochondria are densely packed between the myofibrils (m) and often mitochondrion extent the full length of a sarcomere (m in c, d). Sarcomeres are composed of dark bands (A) and two hemi light bands (I). The center of each A band was occupied by a pale area, the H band (H), which was bisected by a thin (M) line and limited by Z line (Z). Diads (Di) are at the sites of Z lines (c). An intercalated disk (ID) is seen in (a). (Group 1).

Table 1
score grading for semiquantitative evaluation of mitochondrial morphological changes and its % in all groups with the change significance between all groups.

Score	Groups										Kruskal–Wallis test	
	Group 1		Group 2		Group 3		Group 4		Total		X^2	*p*-Value
	N	%	*N*	%	*N*	%	*N*	%	*N*	%		
Grade 0	3	60.00	3	60.00	0	0.00	0	0.00	6	30.00	14.272	0.003*
Grade 1	2	40.00	2	40.00	0	0.00	3	60.00	7	35.00		
Grade 2	0	0.00	0	0.00	2	40.00	2	40.00	4	20.00		
Grade 3	0	0.00	0	0.00	3	60.00	0	0.00	3	15.00		
Total	5	100.0	5	100.0	5	100.00	5	100.00	20	100.00		

	Mann–Whitney test					
Compared groups	1&2	1&3	1&4	2&3	2&4	3&4
p-Value	1.000	0.007*	0.031*	0.007*	0.031*	0.020*

N, number.
* Significant.

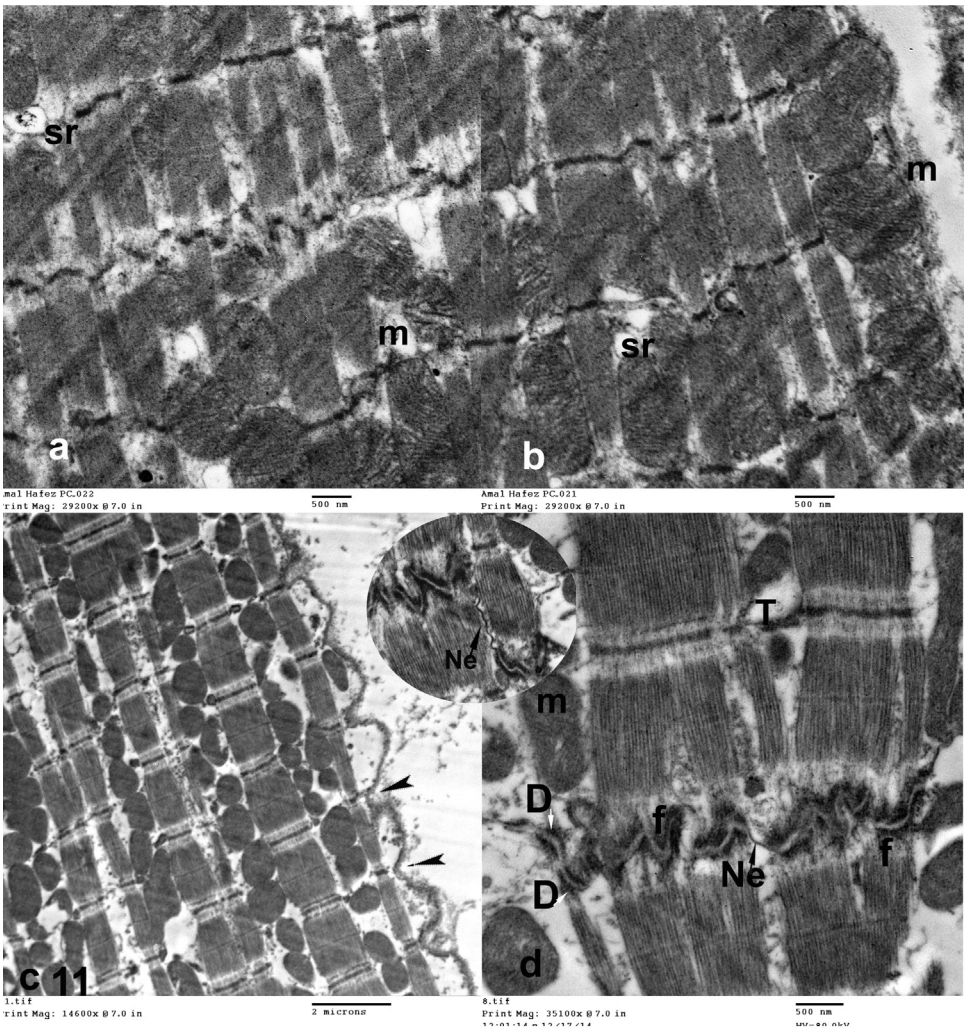

Fig. 11. Electronmicrographs of control left ventricle muscle sections showing mitochondria with numerous closely packed cristae (m) in (a–d). Lace-like profiles of sarcoplasmic reticulum (sr) in (a, b) and parts of T tubules (T) can be identified in (d). An intercalated disk (at the site of Z line) has transverse portions, where fasciae adherents (f) (attach thin myofilaments) and desmosomes (D) are abundant, as well as longitudinal portions rich in gap junctions (Ne) in (d and inset). Sarcolemma is scalloped, forming grooves at the Z lines levels; from which transverse tubules take their origin (arrow heads) in (c). (Groups 1 and 2).

off when vitamin C was added, meanwhilestill significant. Histogram 1 represents mean range of the semiquantitative mitochondrial morphological changes score and the interquartile range.

3.3.2. Optical density statistical analysis for Mallory's trichrome

Statistical analysis for optical density of Mallory's trichrome stained sections showed no significant differences between all groups, where the *p* value was 0.074.

3.3.3. Optical density statistical analysis for caspase 3 reactions

Statistical analysis showed nonsignificant caspase 3 reactions optical density between all groups, in spite of being apparently increased in group 3, where the *p* value was 0.085.

4. Discussion

It is evidence based that the outcome of cardiac ischemic events depends not only on the size, intensity, and duration of the ischemic insult but also, to a large degree, on the native defensive mechanisms of the myocardium itself. These defensive mechanisms provide tolerance to myocardial ischemia/reperfusion as reported by many researchers [20–22] so we can call it as cardiac ischemic tolerance.

Hence, the basal state of cardiac ischemic tolerance and the recruitability of further cardioprotective mechanisms play a major role in determining the damage following an ischemic stimulus. Cardiac ischemic tolerance reflects myocardial functional reserves that are not always used when the tissue is appropriately oxygenated. Ischemic tolerance is modulated by different signal transduction pathways, genetic factors and cellular enzymes, converging on the mitochondria as the main end effector [22]. Therefore,

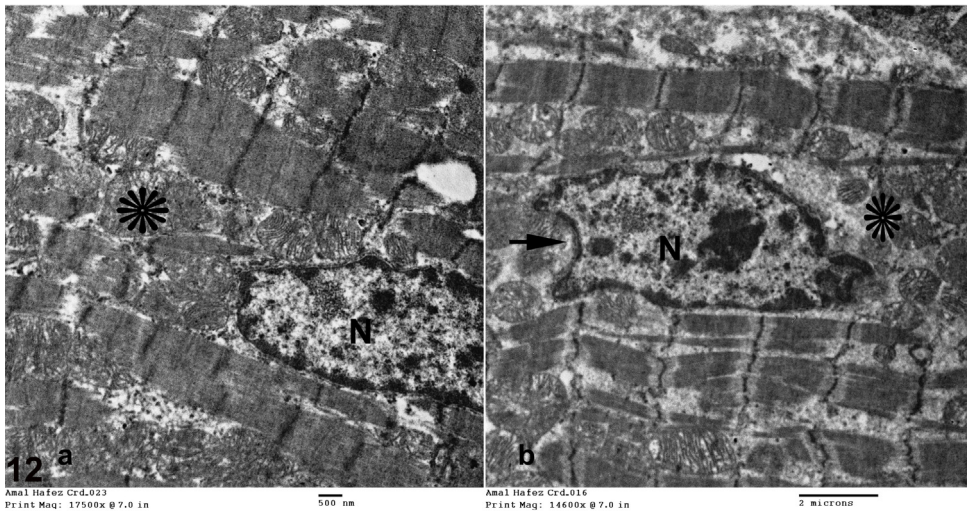

Fig. 12. Electronmicrographs of $KBrO_3$ treated left ventricle muscle sections showing nuclei (N) of two myocytes, in (a) appears irregular while in (b) is deeply indented (arrow) with clumps of heterochromatin in both; and wide juxtanuclear region (stars). (Group 3).

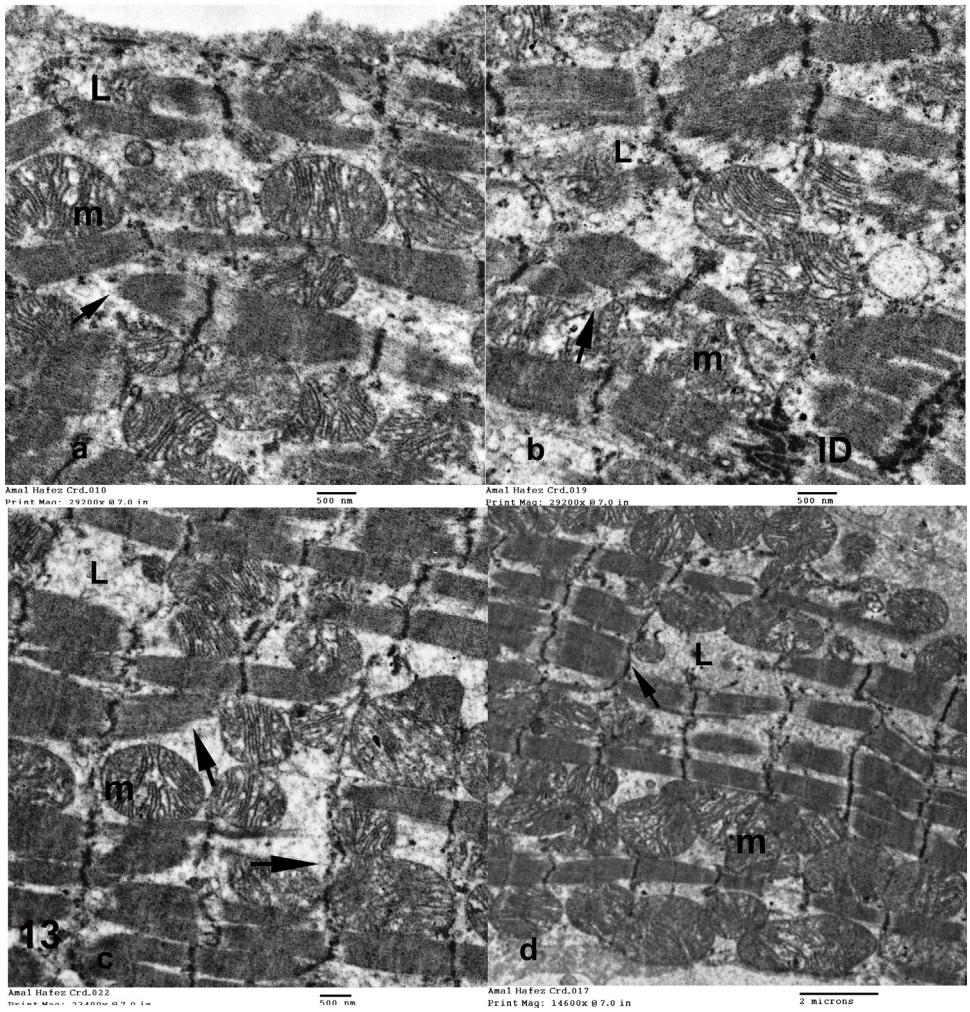

Fig. 13. Electromicrographs of $KBrO_3$ treated left ventricle muscle sections show focal areas of fragmentation and lysis (L) of some myofibrils and disruption of others (arrows) (a–d). Some mitochondria (m) appear with partially destroyed cristea (a–d). (ID) ladder step intercalated disk (b). (Group 3).

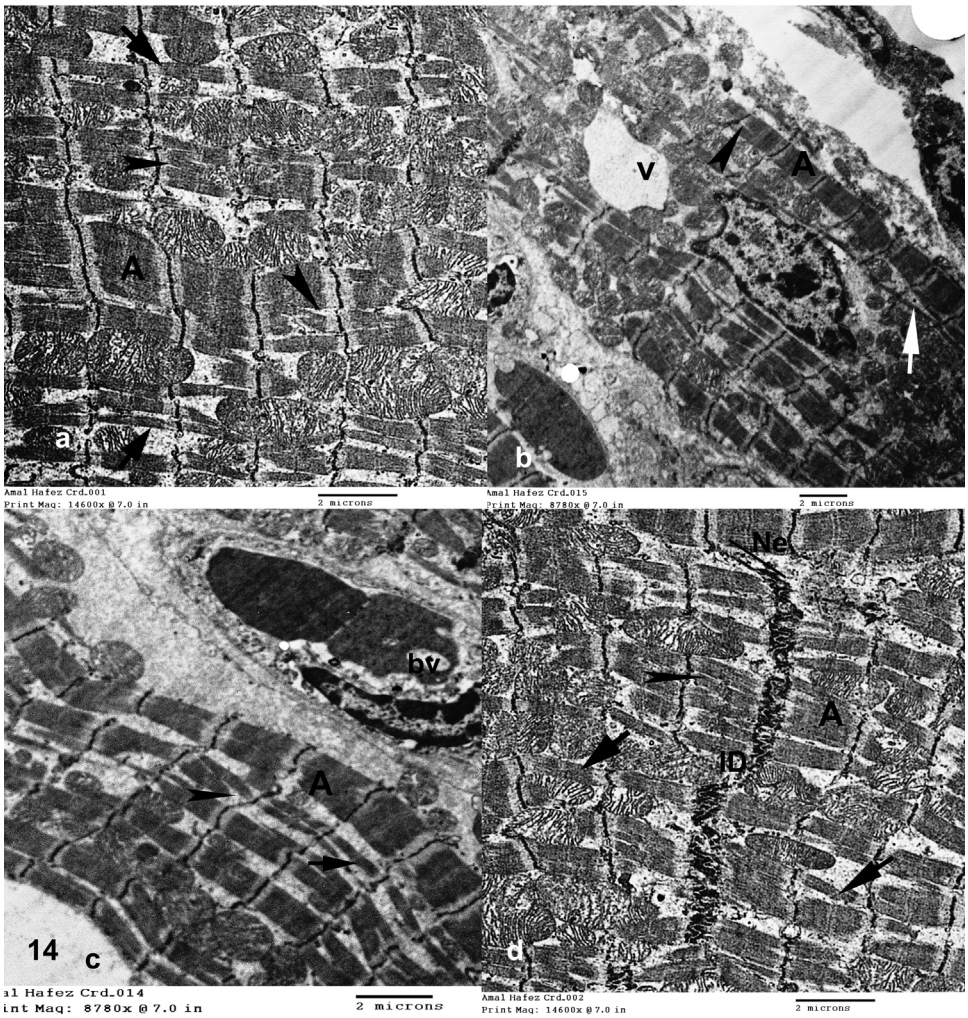

Fig. 14. Electromicrographs of $KBrO_3$ treated left ventricle muscle sections showing loss of the uniform thickness pattern of myofibrils, where some appear very thin (arrows) (a–d), others are average (A) (a, c, d) and several are split (arrow heads) (a–d), huge perinuclear vacuole (v) (b). Blood vessel (bv) in (c), intercalated disk (ID), nexus of longitudinal portion (Ne) in (d) are clear. (Group 3).

drugs and toxins affecting these pathways may impair cardiac ischemic tolerance without affecting myocardial function in oxygenated conditions. Such an effect would not be detected by current toxicological studies but would considerably influence the outcome of ischemic events. Such an effect is referred as "occult cardiotoxicity."

In this work, the authors tried to get evidence that $KBrO_3$ induces occult cardiotoxicity at the level of the cell structure and whether vit. C can protect the cardiac tolerance. The oxidative stress of ($KBrO_3$) promotes oxidative cell damages with injuries in different tissues and organs through reaction with proteins, lipids and nucleic acids; in the course of production of reactive oxygen species (ROS) [23]. As there is a negative balance between oxidative stress damage and antioxidants; the heart tissue is very sensitive to free radical damage because of its high oxidative metabolism and weak antioxidant defense [24].

The semiquantitative evaluation of mitochondrial morphological changes in current work indicated that $KBrO_3$ treated animals proved several alterations which retained to moderate in the speak about vit. C concomitant administration with $KBrO_3$. Mitochondria appeared swollen with irregular shape, size and partially destructed cristae. Central effacement seen in some sections may be due to hyperfolding of the mitochondrial center, so they appeared with empty center on cut sections.

This can be explained by the fact that ROS production by mitochondria can lead to oxidative damage to mitochondrial proteins, membranes and DNA, impairing the ability of mitochondria to synthesize ATP and to carry out their wide range of metabolic functions [13]. In addition, mitochondrial ROS production leads to induction of the mitochondrial permeability transition pore (PTP), which renders the inner membrane permeable to small molecules in situations such as ischemia/reperfusion injury [13]. Consequently, it is unsurprising that mitochondrial oxidative damage contributes to a wide range of pathologies for itself, other cell organelles or even to entire the cell.

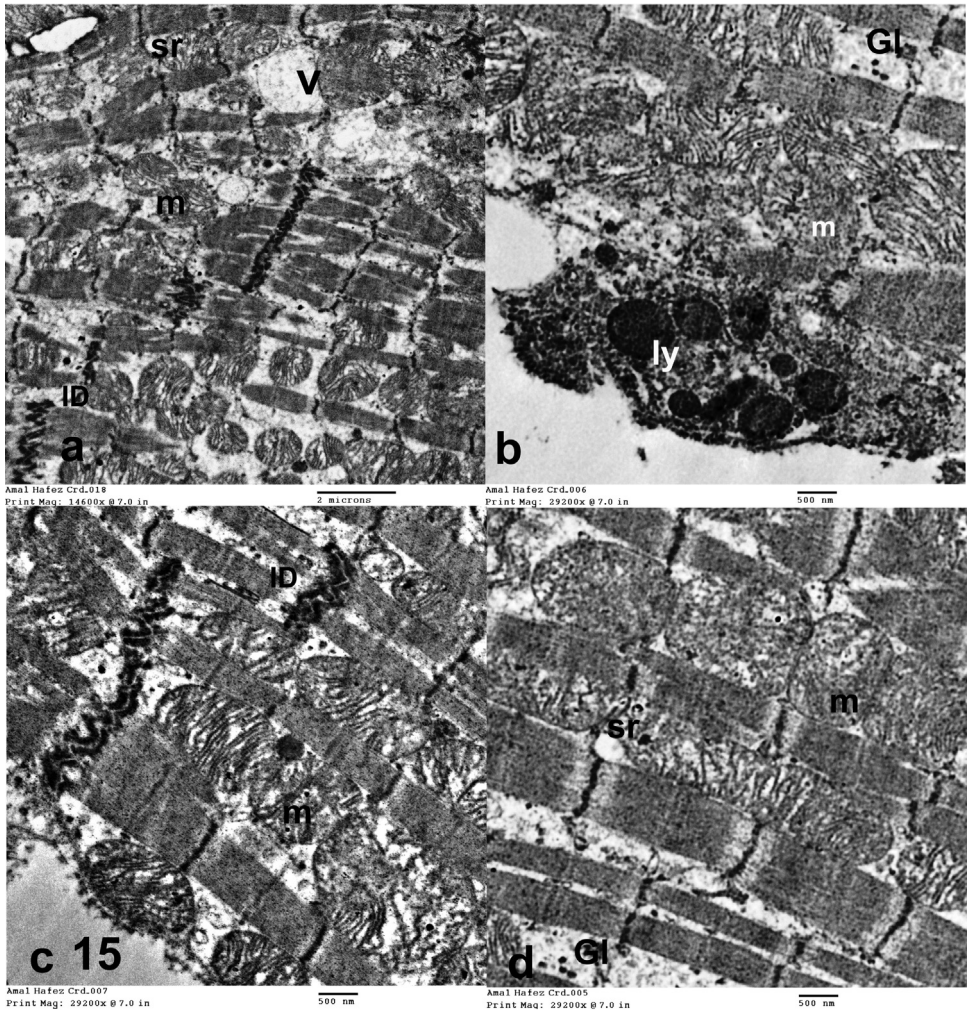

Fig. 15. Electronmicrographs of $KBrO_3$ treated left ventricle muscle sections showing areas of sarcoplasmic vacuolization in between the myofibrils (V) in (a) and in (b) subsarcolemmal lysosomes (ly) are observed. The mitochondria (m) are swollen, with partially destroyed cristae, irregularly arranged with different sizes, and have a heterogenous density of matrix (a–d). Ladder step intercalated disk (ID) in (a, c); sarcoplasmic reticulum (sr) (a, d), glycogen granules (Gl) (b, d) are seen. (Group 3).

In the present research, light microscopic (LM) appearance of some $KBrO_3$ treated cardiomyocytes revealed partially disintegrated or globular cytoplasm, sometimes lost striations. Some authors reported that this myofibrillar injury might be a secondary event after mitochondrial dysfunction, which could lead to an imbalance in calcium uptake and loss of ATP production, resulting in disturbance of normal myofibrillar structure and function [25].

These findings were confirmed by the focal areas of disruption, fragmentation or even lyses of some myofibrils observed in the EM examinations. These changes could be simplified by suggesting degradation of myofibrils as a result of significantly decreased relative contents of myosin heavy chain and alpha-actinin. Similar results were suggested by Maisch et al. [26] in dilated cardiomyopathy. Other expressions of these atypical fibrils seen by EM were in the form of loss of the uniform thickness pattern or split and tear. That may be a consequence of disturbed cell functions (nuclear and sarcoplasmic) causing altered myofilament formation and renewal.

On other respects, although historically viewed as purely harmful, recent evidences suggest that ROS (as members of free radical system) function as important physiological regulators of intracellular signaling pathways [27]. Indeed free radicals are not merely harmful but actually their presence is essential for the cell life. Free radicals are the power against microorganisms, exogenous invaders and so. However their excess in the cell is the start of risk; in addition, mitochondrial ROS may act as a modulatable redox signal, reversibly affecting the activity of a range of functions in the mitochondria, cytosol and nucleus [13]. Accordingly, in the present study, dark, huge and less elongated nuclei by LM, while irregular, deeply indented with clumps of heterochromatin EM pictures of others were elected after $KBrO_3$ management. These alterations are indicative of less active or even ill cells.

"Redox signaling" is the concept that electron-transfer processes play a key messenger role in biological systems. Redox is the portmanteau of reduction and oxidation. Redox signaling occurs when a biological system alters in

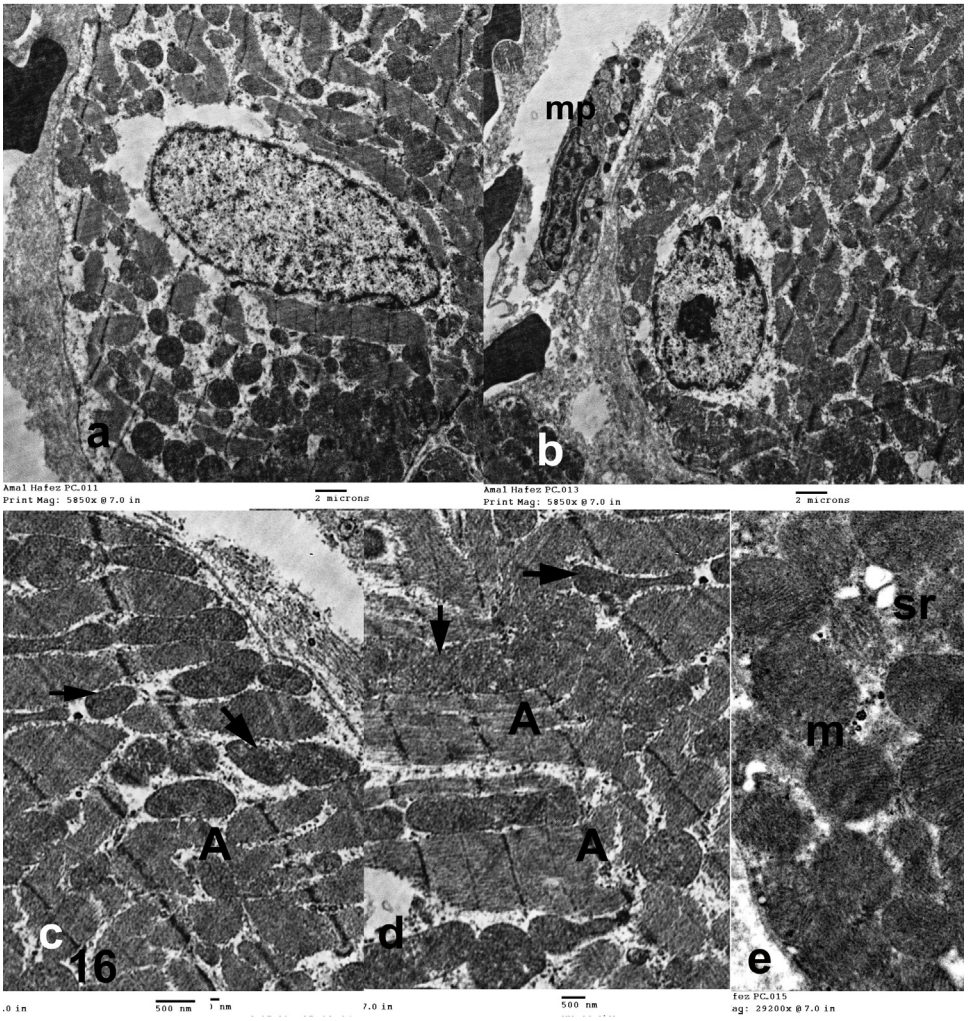

Fig. 16. Electronmicrographs of $KBrO_3$ and vit. C treated left ventricle muscle sections show oval euchromatic nucleus with average juxtanuclear region in (a); slightly irregular nucleus with a prominent nucleolus in (b). The myofibrils were nearly regularly arranged showing an average size (A) and regular striation pattern in (c, d). Mitochondria (m) have intact cristea in (e) and dense matrix, while in (c, d) it is irregularly arranged and has irregular shapes and sizes (arrows). Macrophage (mp) in (b) and (sr) sarcoplasmic reticulum in (e) are seen. (Group 4).

response to a change in the level of ROS. Although excess ROS is best known as damaging agent in pathology, a more accurate view has developed. It is now clear that ROS can act as messengers both in the extracellular environment and within cells [28,29]. So free radical reactions are redox reactions that occur as a part of homeostasis and killing microorganisms. Simply, the redox reactions have replaced the ROS actions.

Mitochondria seem to be an important redox signaling node, partly because of the flux of the ROS superoxide ($O2^{\bullet -}$) [27]. In addition, the mitochondrial matrix is central to metabolism, as oxidative phosphorylation, the citric acid cycle, fatty acid oxidation, the urea cycle and the biosynthesis of iron sulphur centers and heme take place there [27].

The subsequent effects on cell membrane may include an increase in osmotic fragility, an increase in permeability, inactivation of membrane-bound enzymes such as ATPases, and cross-linking of membrane constituents. In this respect also, the formation of vacuoles with increased juxtanuclear paler stained region and nuclear alterations, might be attributed to expansion of cytoplasmic membranous components caused by intracellular water and electrolytes redistribution [30].

Another observation in the present study was the congestion of blood vessels with extravasation of blood cells in between the muscle fibers. Such abnormalities might occur due to microvascular injury as a result of an inflammatory process caused by excessive production of ROS.

The connective tissue cells, matrix and collagen were abundant with $KBrO_3$ treatment. This was evidenced by H&E and Mallory's trichrome stain where it showed increase in its surface area. This could be either due to excessive production of collagen by fibroblasts or due to decreased degradation of collagen by matrix metalloproteinase [31].

Fibroblasts comprise the largest cell population in the myocardium. In heart disease and toxicity, the number of

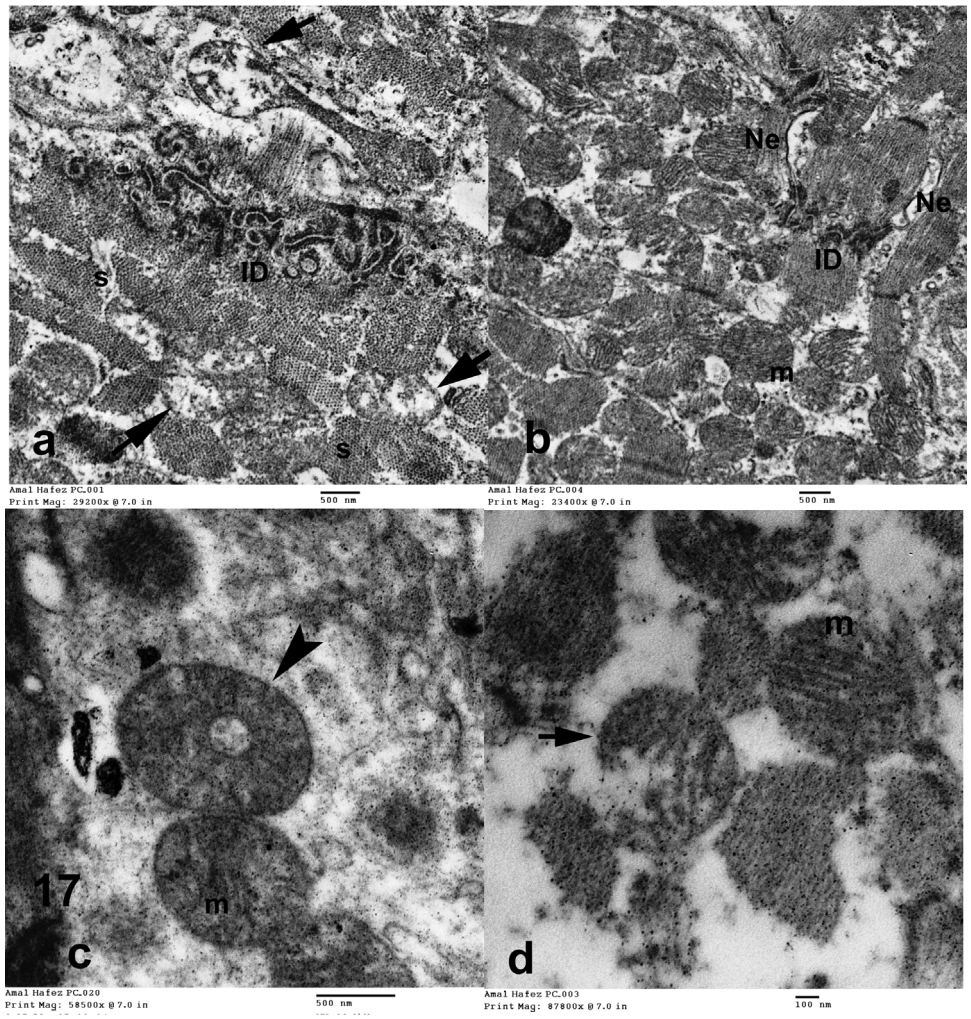

Fig. 17. Electronmicrographs of $KBrO_3$ and vit. C treated left ventricle muscle sections showing intercalated disks (ID) appeared intact in transverse (a) and longitudinal (b) sections; nexus (Ne). Mitochondria have intact cristea and dense matrix (m), while few appear swollen with irregular shape, size and partially destroyed cristae (arrows) in (a–d). Mitochondrion has central effacement (arrow head) (c). The dot-like regular lattice (S) found in (a) are myofibrils in transverse section. (Group 4).

fibroblasts is increased either by replication of the resident myocardial fibroblasts, migration and transformation of circulating bone marrow cells, or by transformation of endothelial/epithelial cells into fibroblasts and myofibroblasts. The primary function of fibroblasts is to produce structural proteins that comprise the extracellular matrix (ECM). This can be a helpful process; however, hyperactivity of cardiac fibroblasts can result in excess production and deposition of ECM proteins in the myocardium, known as fibrosis, with adverse effects on cardiac structure and function. In addition to being the primary source of ECM proteins, fibroblasts produce a number of cytokines, peptides, and enzymes among which matrix metalloproteinases and their inhibitors directly impact the ECM turnover and homeostasis [32].

Despite the background knowledge of the spiral arrangement of muscle fibers [33], remodeling of the ECM is a key component of cardiac remodeling (the changes in size, shape, structure and physiology of the heart after injury to the myocardium) that occurs in disease [34]. Thus, $KBrO_3$ induced ECM expansion and remodeling are indicative of sever toxicity. However its drop off in vitamin C treated animals, points to its prevention from the start.

Fibrillar collagen types I and III are the predominant components of cardiac ECM [33,34]. In the current study, the optical density was done to illuminate any changes in the collagen type, however the nonsignificant changes between the groups point to the existence of the same type of collagen reaction.

The endoplasmic reticulum (ER) is a multifunctional organelle responsible for the synthesis and folding of proteins as well as for signaling and calcium storage, which has been linked to the contraction–relaxation process. Disruptions of its homeostasis activate a stress response. For alterations in ER to happen, its molecular components must be shared [35]. The reticulons are a family of proteins that function mainly to stabilize the curvature of ER tubules [36]. Voeltz et al. have studied the effect of expression

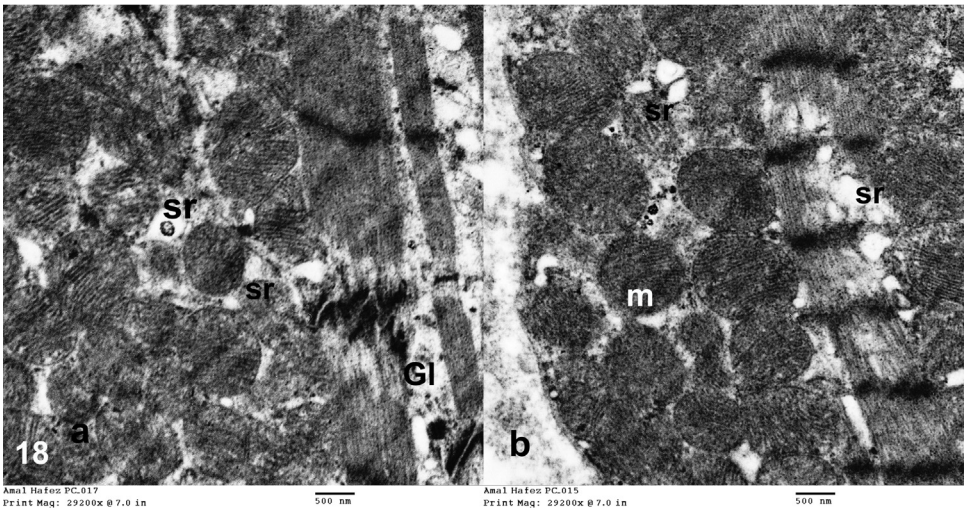

Fig. 18. Electronmicrographs of $KBrO_3$ and vit. C treated left ventricle muscle sections show sarcoplasmic reticulum (sr) within average (a, b) caliber. The mitochondria have intact cristea and dense matrix (m), the glycogen still depleted (Gl) (a, b).

modification of reticulons *in vitro* and found that the down-regulation of Reticulon 1 under stress conditions produces changes in the peripheral ER through the formation of membrane sheets, when the reticulons are overexpressed, tubule formation increases [37]. As there is a specific relationship between ER stress, structure and function, the sarcoplasmic changes found in this work may be due to, or leading to cell stress and damage.

Numerous large mitochondria and glycogen stores are adjacent to each myofibril. Thus, the structures that store energy (glycogen granules) and the structures that release and recapture energy (mitochondria) are located adjacent to the structures (myofibrils) that use the energy to drive contraction. That is why there was stress depletion of the glycogen granules in the present work; in addition juxtanuclear pale stained areas may represent the site of glycogen.

Some specialized intercellular junctions and intercalated discs are present between the ends of adjacent cardiac muscle cells, which not only provide points of anchorage

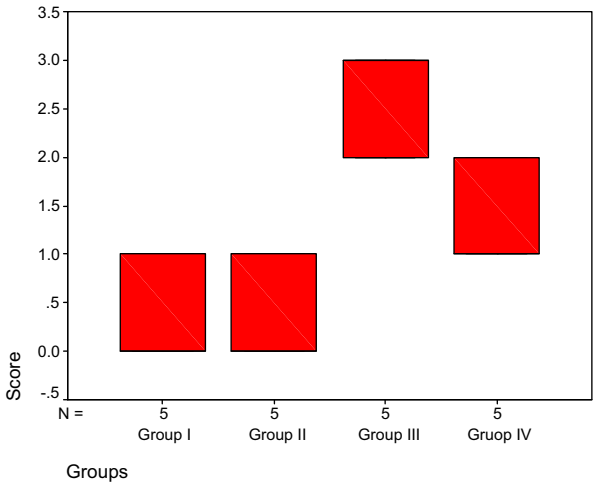

Histogram 1. Mean range of the semiquantitative mitochondrial morphological changes score and the interquartile range.

for the myofibrils but also permit extremely rapid spread of contractile stimuli from one cell to another. Thus, adjacent fibers are triggered to contract almost simultaneously, thereby acting as a functional syncytium. Fascia adherens (adhering junction) are the major constituent of the transverse component of the intercalated disc and are responsible for its staining in routine H&E. Essentially, they represent hemi-Z bands. Intercalated discs have not changed along the groups of this work, but they may be affected in longer durations or higher doses of $KBrO_3$ administration.

It has been long believed that apoptosis does not occur in terminally differentiated cells such as adult cardiomyocytes. However, all mechanisms responsible for induction of apoptosis are running in myocytes and are particularly activated during heart stress or chemical toxicity. Mitochondrial oxidative damage can increase the tendency of mitochondria to release intermembrane space proteins such as cytochrome c (cyt c) to the cytosol by mitochondrial outer membrane permeabilization and thereby activate the cell's apoptotic machinery. Consequently, mitochondria have a key role in caspases induced apoptosis [13,38] that can explain the increased caspase 3 reactions in group 3 in spit of being nonsignificant.

To protect themselves against toxic free radicals, cells develop antioxidant defenses by endogenous enzymatic and/or non-enzymatic components. Though an efficient defense system is present in the cells, it may be overwhelmed under stress conditions [3]. Now that is the time for exogenous antioxidants. Antioxidants work through different mechanisms to prevent oxidant-induced cell damages. They act for redox homeostasis, can reduce the generation of ROS, scavenge them, or interfere with their-induced alterations. As modulating mitochondrial activity is an important possibility to control oxidative stress toxicity, mitochondrial redox signals are produced and modulated, so can alter mitochondrial functions [13].

Vitamin C exerts a protective role, being an essential co-factor for many enzymes and an efficient, even one of

the most efficient antioxidants. Vitamin C reacts directly with superoxide and works for redox homeostasis, now Vitamin C is not merely scavenger but rather exists in the cell as sensor and effector of redox-regulated pathways [39]. Accordingly, when we used vitamin C in parallel with $KBrO_3$, cardiac muscle showed better appearance that focused the light on the role of vitamin C in protection against $KBrO_3$ hazards.

5. Conclusion

These results again underscore the notion that "$KBrO_3$ is considered as a food pollutant not a food additive" evidenced by its injurious histological changes on the left ventricle muscle, causing occult cardiotoxicity. However those alterations could be eliminated through enhancement of cardiac tolerance by concurrent vitamin C administration. Is this in line with "*An ounce of prevention is worth a pound of treatment*"?

Conflict of interest

None declared.

References

[1] Duarte T, Lunec J. Review: when is an antioxidant not an antioxidant? A review of novel actions and reactions of vitamin C. Free Radic Res 2005;39(7):671–86.
[2] Rekha C, Poornima G, Manasa M, Abhipsa V, Devi JP, Kumar HTV, et al. Ascorbic acid, total phenol content and antioxidant activity of fresh juices of four ripe and unripe citrus fruits. Chem Sci Trans 2012;1(2):303–10.
[3] Kucharski H, Zajac J. Handbook of vitamin C research. Daily requirements, dietary sources and adverse effects. Nova; 2010. p. 65.
[4] Ueno H, Oishi K, Sayato Y, Nakamuro K. Oxidative cell damage in Kat-sod assay of oxyhalides as inorganic disinfection by-products and their occurrence by ozonation. Arch Environ Contam Toxicol 2000;38(1):1–6.
[5] Parsons JL, Chipman JK. The role of glutathione in DNA damage by potassium bromate in vitro. Mutagenesis 2000;15(4):311–6.
[6] Sai K, Hayashi M, Takagi A, Hasegawa R, Sofuni T, Kurokawa Y. Effects of antioxidants on induction of micronuclei in rat peripheral blood reticulocytes by potassium bromate. Mutat Res 1992;269(1):113–8.
[7] Watanabe S, Togashi S, Fukui T. Contribution of nitric oxide to potassium bromate-induced elevation of methaemoglobin concentration in mouse blood. Biol Pharm Bull 2002;25(10):1315–9.
[8] Achukwu PU, Ufelle SA, Ukaejiofo EO, Ejezie FE, Nwachukwu DN, Nwagha UI, et al. The effect of potassium bromate on some haematological parameters of Wistar rats. Niger J Physiol Sci 2009;24(1):59–61.
[9] Kujawska M, Ignatowicz E, Ewertowska M, Adamska T, Markowski J, Jodynis-Liebert J. Attenuation of $KBrO_3$-induced renal and hepatic toxicity by cloudy apple juice in rat. Phytother Res 2013;27(8):1214–9.
[10] Kurokawa Y, Maekawa A, Takahashi M, Hayashi Y. Toxicity and carcinogenicity of potassium bromate – a new renal carcinogen. Environ Health Perspect 1990;87:309–35.
[11] DeAngelo AB, George MH, Kilburn SR, Moore TM, Wolf DC. Carcinogenicity of potassium bromate administered in the drinking water to male B6C3F1 mice and F344/N rats. Toxicol Pathol 1998;26(5):587–94.
[12] Shimura S, Matsui Y, Yutani C, Suto Y, Akashi O, Matsui K, et al. Histopathological study of specimens obtained by left ventricular biopsy during ventriculoplasty for idiopathic dilated cardiomyopathy. Tokai J Exp Clin Med 2009;34(1):1–7.
[13] Murphy MP. How mitochondria produce reactive oxygen species. Biochem J 2009;417(1):1–13.
[14] Khan N, Sharma S, Sultana S. *Nigella sativa* (black cumin) ameliorates potassium bromate-induced early events of carcinogenesis: diminution of oxidative stress. Hum Exp Toxicol 2003;22(4):193–203.
[15] Suvarna SK, Layton C, Bancroft JD. Bancroft's theory and practice of histological techniques. 7th ed. Elsevier Limited; 2013. p. 105–65.
[16] Bozzola JJ, Russell LD. Electron microscopy. 2nd ed. USA: Jones and Bartlett; 1999, 17 p.
[17] Burniston JG, Tan LB, Goldspink DF. Relative myotoxic and haemodynamic effects of the beta-agonists fenoterol and clenbuterol measured in conscious unrestrained rats. Exp Physiol 2006;91(6):1041–9.
[18] Burniston JG, Saini A, Tan LB, Goldspink DF. Angiotensin II induces apoptosis in vivo in skeletal, as well as cardiac, muscle of the rat. Exp Physiol 2005;90(5):755–61.
[19] Bishop JB, Tani Y, Witt K, Johnson JA, Peddada S, Dunnick J, et al. Mitochondrial damage revealed by morphometric and semiquantitative analysis of mouse pup cardiomyocytes following in utero and postnatal exposure to zidovudine and lamivudine. Toxicol Sci 2004;81(2):512–7.
[20] Ravingerova T. Intrinsic defensive mechanisms in the heart: a potential novel approach to cardiac protection against ischemic injury. Gen Physiol Biophys 2007;26(1):3–13.
[21] Peart JN, Headrick JP. Sustained cardioprotection: exploring unconventional modalities. Vasc Pharmacol 2008;49(2/3):63–70.
[22] Golomb E, Nyska A, Schwalb H. Occult cardiotoxicity – toxic effects on cardiac ischemic tolerance. Toxicol Pathol 2009;37(5):572–93.
[23] Farombi EO, Alabi MC, Akuru TO. Kolaviron modulates cellular redox status and impairment of membrane protein activities induced by potassium bromate (KBrO(3)) in rats. Pharmacol Res 2002;45(1):63–8.
[24] Yilmaz S, Atessahin A, Sahna E, Karahan I, Ozer S. Protective effect of lycopene on adriamycin-induced cardiotoxicity and nephrotoxicity. Toxicology 2006;218(2/3):164–71.
[25] Zhou S, Starkov A, Froberg MK, Leino RL, Wallace KB. Cumulative and irreversible cardiac mitochondrial dysfunction induced by doxorubicin. Cancer Res 2001;61(2):771–7.
[26] Maisch B, Richter A, Sandmoller A, Portig I, Pankuweit S. Inflammatory dilated cardiomyopathy (DCMI). Herz 2005;30(6):535–44.
[27] Finkel T. Signal transduction by reactive oxygen species. J Cell Biol 2011;194(1):7–15.
[28] Kelkka T, Kienhofer D, Hoffmann M, Linja M, Wing K, Sareila O, et al. Reactive oxygen species deficiency induces autoimmunity with type 1 interferon signature. Antioxid Redox Signal 2014;21(16):2231–45.
[29] Janssen-Heininger YM, Mossman BT, Heintz NH, Forman HJ, Kalyanaraman B, Finkel T, et al. Redox-based regulation of signal transduction: principles, pitfalls, and promises. Free Radic Biol Med 2008;45(1):1–17.
[30] Balli E, Mete UO, Tuli A, Tap O, Kaya M. Effect of melatonin on the cardiotoxicity of doxorubicin. Histol Histopathol 2004;19(4):1101–8.
[31] Westermann D, Rutschow S, Jager S, Linderer A, Anker S, Riad A, et al. Contributions of inflammation and cardiac matrix metalloproteinase activity to cardiac failure in diabetic cardiomyopathy: the role of angiotensin type 1 receptor antagonism. Diabetes 2007;56(3):641–6.
[32] Weber KT, Pick R, Janicki JS, Gadodia G, Lakier JB. Inadequate collagen tethers in dilated cardiopathy. Am Heart J 1988;116(6 Pt 1):1641–6.
[33] Buckberg G, Hoffman JI, Mahajan A, Saleh S, Coghlan C. Cardiac mechanics revisited: the relationship of cardiac architecture to ventricular function. Circulation 2008;118(24):2571–87.
[34] Fan D, Takawale A, Lee J, Kassiri Z. Cardiac fibroblasts, fibrosis and extracellular matrix remodeling in heart disease. Fibrogenesis Tissue Repair 2012;5(1):15.
[35] Ortega A, Rosello-Lleti E, Tarazon E, Molina-Navarro MM, Martinez-Dolz L, Gonzalez-Juanatey JR, et al. Endoplasmic reticulum stress induces different molecular structural alterations in human dilated and ischemic cardiomyopathy. PLOS ONE 2014;9(9):e107635.
[36] Hu J, Shibata Y, Voss C, Shemesh T, Li Z, Coughlin M, et al. Membrane proteins of the endoplasmic reticulum induce high-curvature tubules. Science (New York, NY) 2008;319(5867):1247–50.
[37] Voeltz GK, Prinz WA, Shibata Y, Rist JM, Rapoport TA. A class of membrane proteins shaping the tubular endoplasmic reticulum. Cell 2006;124(3):573–86.
[38] Wilson KP, Black JA, Thomson JA, Kim EE, Griffith JP, Navia MA, et al. Structure and mechanism of interleukin-1 beta converting enzyme. Nature 1994;370(6487):270–5.
[39] Giampieri F, Alvarez-Suarez JM, Mazzoni L, Forbes-Hernandez TY, Gasparrini M, Gonzalez-Paramas AM, et al. Polyphenol-rich strawberry extract protects human dermal fibroblasts against hydrogen peroxide oxidative damage and improves mitochondrial functionality. Molecules (Basel, Switzerland) 2014;19(6):7798–816.